

Current measurements over the western continental shelf of India

SATHEESH C. SHENOI* and M. K. ANTONY*

(Received 28 November 1989; accepted 2 April 1990)

Abstract—Current meter observations obtained from a site off Goa ($15^{\circ}08'N$, $73^{\circ}16'E$) over the western continental shelf of India are presented. Data were collected from the site during three different months in a water column of depth about 100 m. The nature of flows are described by means of visual display, linear regression and spectral analysis. The flows are a result of the superimposition of oscillations of wide-ranging frequencies over a weak mean flow. The mean flow was towards south during May and March and towards north during November. The spectral analysis indicates that the inertial and semidiurnal frequency motions are the major contributors to the current structure. The inertial currents were concentrated near the surface with a rapid decay towards the bottom. The analysis also indicates that the diurnal and semidiurnal motions are mainly due to baroclinic internal tides rather than due to barotropic surface tides. Above the semidiurnal frequencies the currents were composed mainly of high-frequency oscillations of comparatively low magnitudes. These motions are strongly time-dependent and they may be related to internal waves in coastal waters.

INTRODUCTION

CURRENTS over the western continental shelf of India have been inferred mainly from observations of physical and chemical seawater properties. While these techniques provide estimates of the mean and very low frequency circulation, direct measurements are required to determine higher frequency time-dependent motion. Very few direct measurements have been reported in the literature. VARKEY (1980) found high tidal influences in a series of current measurements made near Bombay ($19^{\circ}30'N$, $71^{\circ}30'E$).

Because of the scarcity of information on the time-dependent current data on the western continental shelf of India, the described measurements were made. The objective of the experiment was to measure the currents over the shelf for time periods of several inertial cycles. The experiment was not designed as a small-scale study of high-frequency internal wave characteristics. This paper provides a general description of the measured currents off Goa over the western continental shelf of India and representative examples of the analytical results. Part of this data (current observations during May 1984) was also used in the work of SHENOI *et al.* (1988) for the study of flows in the semidiurnal band. For the semidiurnal band, they found that the cross-shore velocities have primarily resulted from the incidence of internal modes, thereby directing their energy towards the shore, and the longshore currents on the other hand are controlled mainly by the processes such

*National Institute of Oceanography, Dona-Paula, Goa 403 004, India.

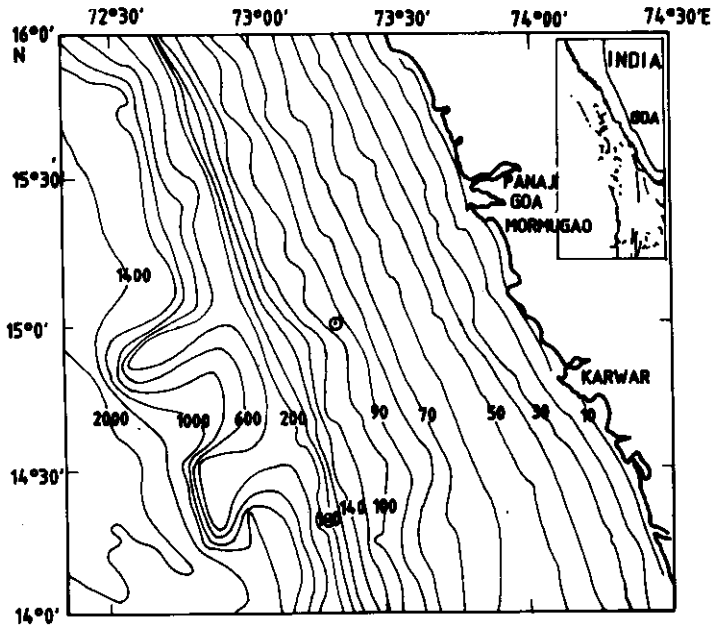


Fig. 1. Bathymetry and location of current meter mooring.

as surface tides which are independent of baroclinic modes. The computation of semidiurnal characteristics from the hydrographic data have confirmed the generation of semidiurnal internal tides along the continental slope and its propagation towards the shore. In this work, we shall highlight the main features of flows observed at a station near Goa using three sets of mooring data collected during three different months.

DESCRIPTION OF MEASUREMENTS

Current measurements were made off the coast of Goa in 92 m water depth during three different months. The mooring site and the bathymetric features of the region are shown in Fig. 1. Aanderra current meters, set at 5 min sampling intervals, were deployed at depths ranging from 10 to 82 m. Details of observation period and data return from each current meter are summarized in Table 1. Data from some of the current meters are not described in this paper, either because of failure of the instrument or because of the limited number of usable records due to obstructions created by fouling animals on the rotor. Thus, from 15 current meters deployed data from only 11 meters could be used. U-mooring was employed for all the deployments with the array supported by a subsurface buoy at a depth of 5 m.

DATA ANALYSIS AND RESULTS

The current observations are analysed by means of visual display, simple statistics, simple linear regression, and spectral analysis. Initially, all 5 min interval current speed and direction values were resolved into on/offshore (U) and alongshore (V) components. These coordinates differ by about 20° from true north. To obtain an initial description of

Table 1. Details of current meter moorings

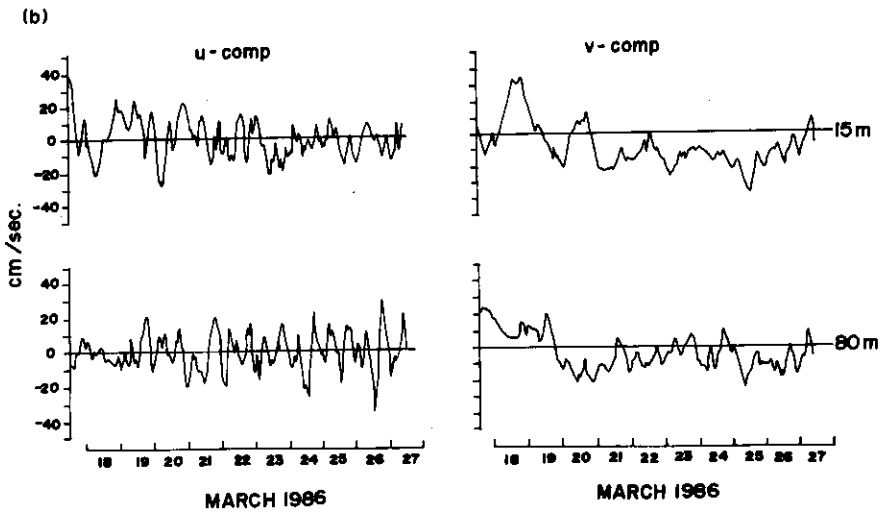
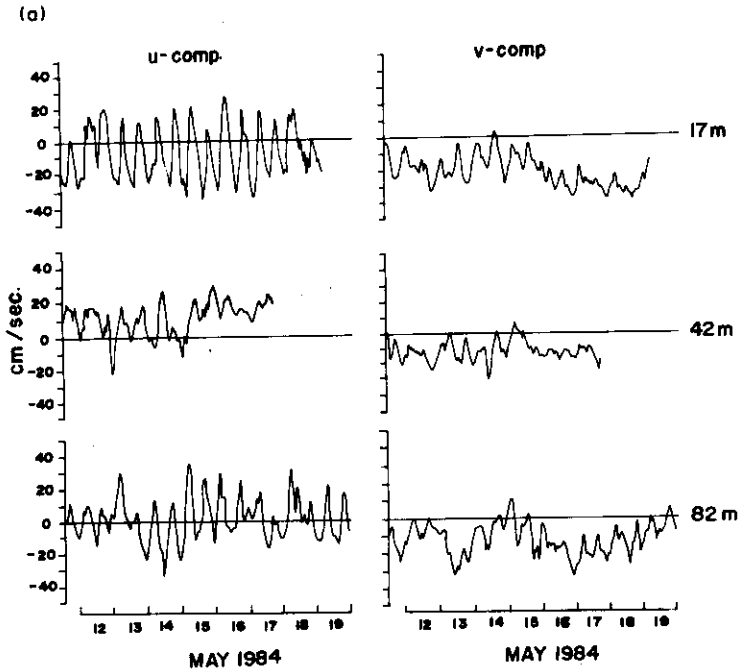
Mooring	Date	Depth of current meter (m)	Duration of usable records (h)
A	11-19 May 1984	17	188
		27	-
		42	156
		62	-
		82	204
B	17-27 Mar. 1986	15	240
		25	-
		40	240
		60	240
		80	240
C	29 Oct.-11 Nov. 1986	10	312
		25	312
		40	276
		60	-
		80	312

the current velocity field, the individual components were averaged to provide hourly current components which are plotted as a function of time (Fig. 2a-c).

Plots indicate that the maximum contribution towards the observed currents are from the time-dependent oscillatory flows with more than one frequency. These oscillations have maximum magnitude at the top current meter (20-25 cm s⁻¹ during May and March and 35-40 cm s⁻¹ during November). Although some records depict a slight increase in speed in the interior of the water column, the current components were generally characterized by a gradual decrease in amplitude with depth. The easily identifiable frequencies of oscillations of the flow components are the semidiurnal and the local inertial frequencies (~46.5 h). The inertial period oscillations have maximum amplitude at the top current meter, whereas the semidiurnal frequency oscillations have the same or even greater magnitudes towards the interior of the water column.

Some of the cross-shore (*U*) components, e.g. top current meters of the March and November set of moorings, have an onshore component that is nearly zero. Others have onshore (e.g. middle current meter of May) or offshore (e.g. top current meter of May and bottom current meter of November) mean flows. Similarly, the alongshore (*V*) components have southward (for all current meters during May and March) and northward (for all current meters during November) mean flows. Alongshore components of large-scale circulation along the west coast of India also indicate a southerly component during March to September and a northerly component during November to January (SHETYE and SHENOI, 1988). The mean southerly component observed during May and March and the northerly component observed during November might be a contribution of the seasonally reversing coastal currents along the west coast of India.

A special feature of the coastal current off the west coast of India is its seasonality associated with the monsoons. During the northeast monsoon (November-February) the winds in the coastal region off western India are generally equatorward with monthly-



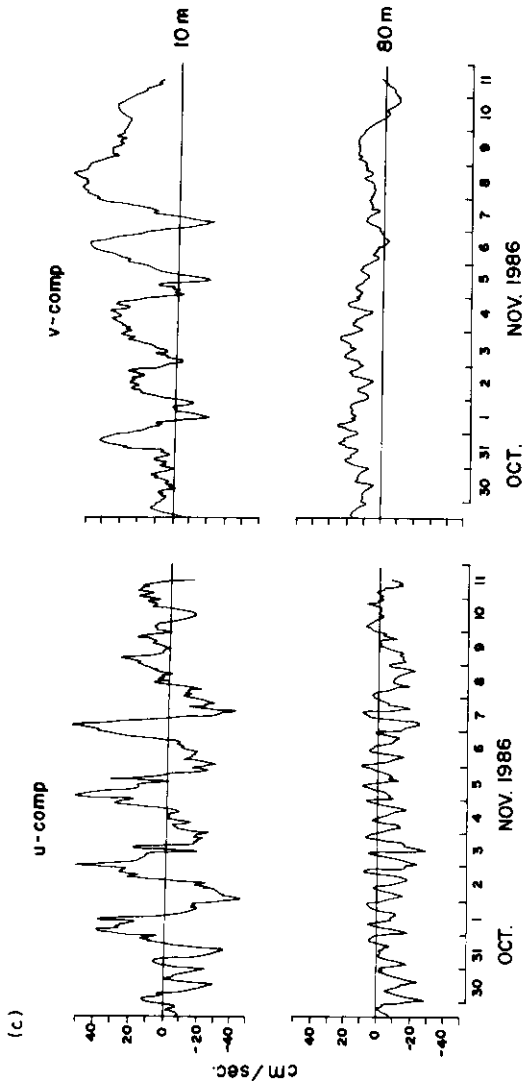


Fig. 2. Time series of hourly current components for (a) May 1984, (b) March 1986 and (c) November 1986.

mean wind speed of approximately 3 m s^{-1} (HASTENRATH and LAMB, 1979). At this time a coastal current flows poleward along the coast. During the rest of the year the coastal current flows with the longshore component of the winds. On the basis of hydrographic observations, SHETYE *et al.* (1990a) have concluded that the circulation off the west coast of India during the southwest monsoon is dynamically similar to the wind-driven eastern boundary currents found elsewhere in the oceans. The northerly flow during the northeast monsoon season appears to be driven by the longshore pressure gradients similar to that of the Leeuwin current (SHETYE *et al.*, 1990b). During the northeast monsoon season the longshore pressure gradients overwhelm the weak longshore winds to drive a northerly current.

Simple statistics of the currents and their components for all three sets of current meter mooring are shown in Table 2. The mean current speeds were relatively low during March compared to the current speeds during May and November. At all levels, the mean flow was southward during May and March and northward during November. The mean V components were stronger than the mean U components. The low magnitudes of mean U components indicate their strong dependence on the time-dependent oscillatory flows compared to the V components. The standard deviations of U components are considerably larger than their mean. In most cases the standard deviations are greater than the mean U components by one order of magnitude. Thus it is obvious that the cross-shore velocities have primarily resulted from the time-dependent oscillatory flows such as local inertial oscillations, diurnal tides, semidiurnal tides, internal waves, etc. The alongshore velocities on the other hand are the result of a mean flow superimposed with time-dependent oscillatory flows.

Regression analysis

The results of linear regression and correlation coefficients computed for both U and V components of each pair of current meters are shown in Table 3. The probability of uncorrelated populations having a correlation coefficient greater than 0.146 is less than 1% for the present sample size (Crow *et al.* 1960).

Table 2. Average current values. $\langle S \rangle$, $\langle \theta \rangle$ mean speed and direction computed from vector components. U , V means and S_u , S_v standard deviations of current components

Period	Depth (m)	$\langle S \rangle$ (cm s ⁻¹)	$\langle \theta \rangle$	U (cm s ⁻¹)	V (cm s ⁻¹)	S_u (cm s ⁻¹)	S_v (cm s ⁻¹)
May 1984	17	23.1	195.8	-6.29	-22.23	15.32	9.34
	42	16.2	130.4	10.52	-12.38	8.99	6.35
	82	12.6	94.5	0.99	-12.52	12.81	8.81
Mar. 1986	15	8.9	94.7	0.7	-8.80	11.28	4.22
	40	5.4	133.5	3.7	-3.90	9.74	2.03
	60	1.4	82.6	1.4	1.20	8.68	9.73
	80	3.1	99.8	0.5	-3.00	10.13	2.11
Nov. 1986	10	21.4	2.2	0.8	21.40	19.04	8.38
	25	13.0	5.0	1.1	12.90	9.58	7.96
	40	8.9	3.9	0.6	8.90	7.52	6.95
	80	12.5	296.6	-5.6	11.10	7.91	7.37

The correlation coefficients are greater and significant at the 99% level between V components for all pairs of current meter. However, they do not show consistency with depth. The correlation coefficients for U components are lower than those for V components and in most cases they are not significant.

The regression equation used for the computation is $V_2 = A_0 + A_1 V_1$, where V_1 is the velocity at the upper current meter and V_2 the velocity at the lower current meter for each pair. If the observed current fluctuation field were barotropic and homogeneous, the correlation coefficient (R) between a pair of current meters would be a function of the separation between them in addition to a near-unity value for regression coefficient A_1 . Instead, our computations show poor correlations, especially between U components, and a regression coefficient A_1 of less than 0.45. This encourages us to conclude that the cross-shore current fluctuation field over the shelf off Goa is primarily baroclinic.

Energy spectra

Rotary spectra were determined using techniques that have been described by GONELLA (1972). The advantage of rotary spectra over ordinary spectra is that it will show not only at which frequency the energy peak occurs but also whether the current at a particular frequency is nearly circular or linear and whether it rotates clockwise or anticlockwise. Individual Fourier coefficients were obtained using the complex fast Fourier transform on current records.

The kinetic energy spectra are generally expected to contain peaks at inertial, diurnal, semidiurnal and higher frequency bands. Frequency bands were selected to place inertial, diurnal and semidiurnal frequencies near centres of separate frequency bands for most of the current records. In addition, two higher frequency bands, HF1 and HF2, were identified for description. Frequencies above 0.4 cph are not discussed as they contain very low energy. Moreover, the probability of noise introduced at these frequencies due to mooring motion, etc. is likely to be high (HALPERN *et al.*, 1974).

The horizontal kinetic energy spectra (clockwise and anticlockwise) for some of the current meters are shown in Fig. 3. The spectra of all the current records are characterized by peaks at local inertial, diurnal and semidiurnal frequencies. Of these three peaks,

Table 3. Correlation coefficient (R) and regression coefficients (A_0 and A_1) between pairs of current meters for U and V components

Period	Depth (m)	Depth (m)	R		A_0		A_1	
			U	V	U	V	U	V
May 1984	17	42	0.09	0.37	11.5	-6.9	0.140	0.274
	17	82	-0.12	0.47	-0.2	-2.7	-0.184	0.441
Mar. 1986	15	40	0.05	0.31	3.7	-1.6	0.039	0.264
	15	60	-0.01	0.43	1.4	2.8	-0.006	0.293
	15	80	-0.13	0.40	0.7	-0.2	-0.295	0.313
Nov. 1986	10	25	0.22	0.41	1.0	7.3	0.110	0.265
	10	40	-0.17	0.18	0.7	8.1	-0.102	0.038
	10	80	-0.17	-0.23	-5.5	13.1	-0.111	-0.094

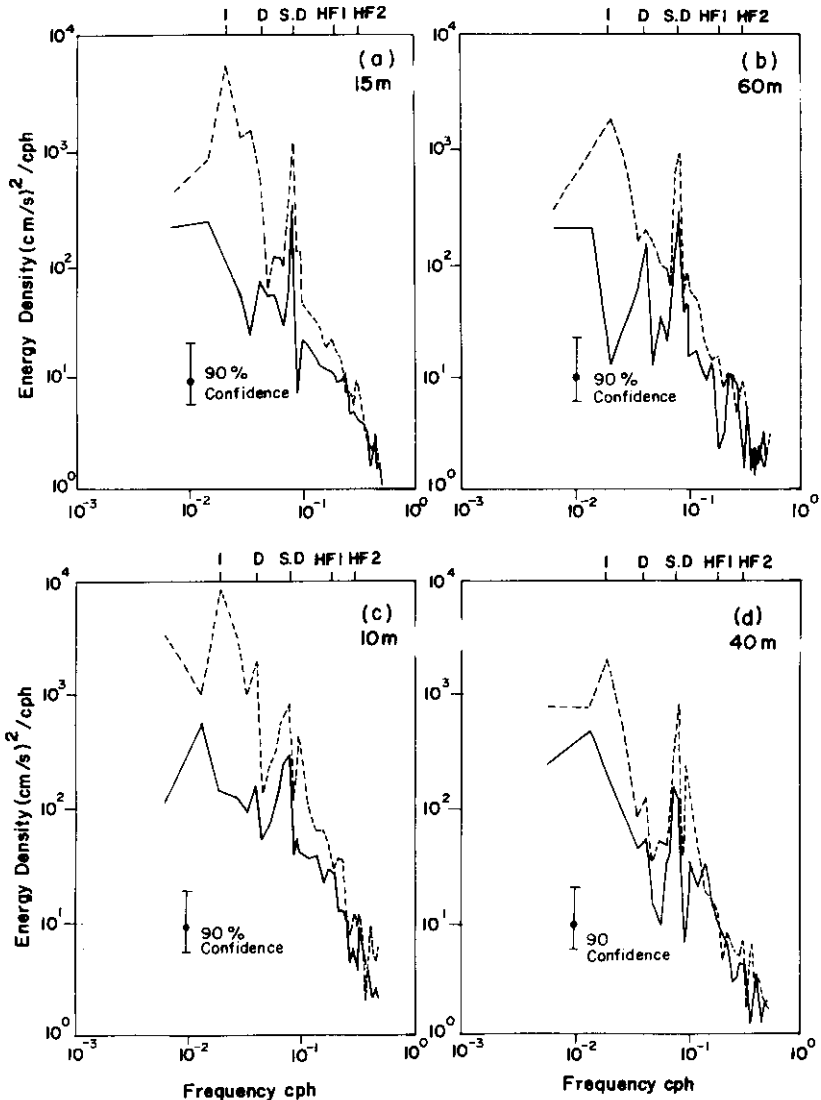


Fig. 3. Horizontal kinetic energy spectra for (---) clockwise and (—) anticlockwise components of currents during March 1986 (a-b) and November 1986 (c-d). The central frequencies of inertial, diurnal, semidiurnal, high frequency 1 and high frequency 2 bands are marked as I, D, SD, HF1 and HF2, respectively. Current meter depths are indicated at top right corner.

greatest energy occurs either at local inertial or at semidiurnal frequency. The spectra of surface current records obtained during March and November show highest energy at the local inertial frequency band and the spectra of records during May show highest energy at the semidiurnal band. In most cases the semidiurnal bands show higher energy than the diurnal band. Beyond the semidiurnal band the higher frequencies, especially frequencies greater than 0.1 cph, are characterized by a sudden drop in energy level, at least by one order of magnitude.

Depth variation of kinetic energy

Band averages were computed over corresponding bands within each section of current record to represent the vertical structure of horizontal kinetic energy. The band width, number of degrees of freedom and the 80% confidence interval for each band are listed in Table 4. The depth variations of the horizontal kinetic energy density (total) for five frequency bands are shown in Fig. 4. The vertical distribution of horizontal kinetic energy in each band is described below.

Inertial band. The distribution of horizontal kinetic energy in this band shows maximum energy at the top current meter and minimum energy at the bottom current meter in all three sets of observations. However, it may be noticed that this energy is largely confined to the upper 40 m of the water column. The inertial energy was at its maximum during the

Table 4. Frequency bands, degrees of freedom and 80% confidence interval limits

Bands	Limits (cph)	C.F. (cph)	80% confidence limits		df
			L	U	
Inertial	0.0139-0.0278	0.0208	0.60	2.60	8
Diurnal	0.0347-0.0486	0.0417	0.60	2.60	8
Semidiurnal	0.0694-0.0972	0.0833	0.68	1.60	16
HF1	0.1111-0.2083	0.1597	0.73	1.45	32
HF2	0.2153-0.4028	0.3056	0.78	1.35	48

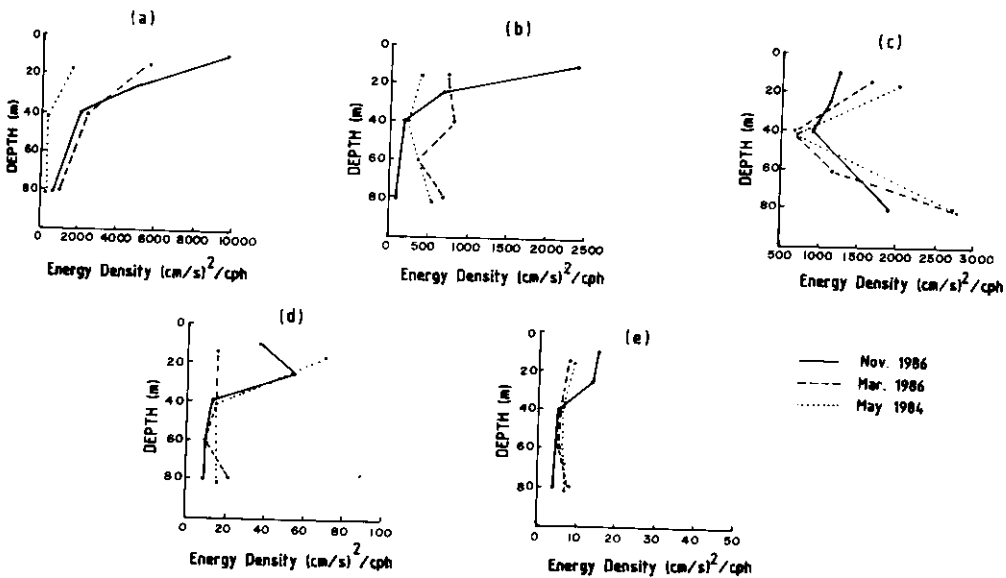


Fig. 4. Depth variation of horizontal kinetic energy density: (a) inertial, (b) diurnal, (c) semidiurnal, (d) high frequency 1 and (e) high frequency 2 bands.

November set of observations and yielded a rapid decay within the upper half of the water column. Similarly, energy in the inertial band during the May and March observations also showed rapid decay within the upper half of the water column. These observations are similar to those of POLLARD and MILLARD (1970) and HAYES and HALPERN (1976). Additionally, the model of POLLARD (1970) also shows a rapid decay of the inertial energy in stratified water.

An inertially rotating wind vector would generate an inertial current of continuously increasing amplitude, as it would always be adding momentum to it. But, a wind vector acting in one direction for one inertial period would generate no inertial current, since it would remove as much momentum in the second half period as it added in the first (POLLARD and MILLARD, 1970). Thus, for an effective generation of inertial motions the wind stress variation must be short compared to the inertial period (half or less than half of the inertial period). The land-sea breeze system prevailing along the west coast of India with a diurnal periodicity, especially during the non-southwest monsoon months, could be a potential candidate for the generation of inertial oscillations at this location as wind vectors vary its direction every 12 h. Except during June to September (southwest monsoon) the land-sea breeze circulation off Goa possesses fairly strong magnitudes of the order of $10\text{--}20\text{ m s}^{-1}$ (MURTY, 1977). It is possible that the greater response observed in the inertial band in November is due to the strong land-sea breeze circulation. The maximum values observed at the surface (for all three sets) indicate that the inertial motions are forced by the winds. The inertial motions forced by the wind, resulting in maximum values near the surface, were also observed off the coast of Peru ($15^{\circ}30'S$) by JOHNSON (1981). The data on frequency and amplitude composition of the winds over the west coast of India are inadequate at present to ascertain whether there was some reinforcement between the diurnal and inertial frequencies.

Diurnal and semidiurnal bands. The main source of diurnal and semidiurnal energy is the barotropic surface tide itself. If the energy observed was only due to the surface barotropic tide, the horizontal kinetic energy would show a constant magnitude throughout the water column, except possibly near the bottom where friction may weaken the currents. The kinetic energy for the diurnal and semidiurnal bands neither shows a constant magnitude throughout the water column nor a consistency with depth. This behaviour is likely to be due to the generation of diurnal internal tides associated with barotropic tidal current flow over the continental shelf break or slope region. The mechanism for generation and propagation of internal tides due to interaction of barotropic tides with bottom topography (shelf) is well known (BAINES, 1973; PRINSBERG and RATTRAY, 1975; SANDSTROM, 1976). The internal waves generated at the shelf break or over the shelf are expected to propagate in an onshore direction as a beam centred about the shoreward characteristic that intersects the shelf break and reflects from the surface and bottom. The characteristics are collinear with the group velocity, and thus, with energy flux; i.e. energy propagates along the characteristics that are lines of constant phase. All available models on generation and propagation of internal tides predict horizontal baroclinic velocities as large or larger than barotropic velocities in the vicinity of the characteristic.

The barotropic and baroclinic components of velocities were separated in the semidiurnal band (SHENOI *et al.*, 1988) for the set of current records obtained during May. The baroclinic component was larger (almost double at the top and bottom current meters)

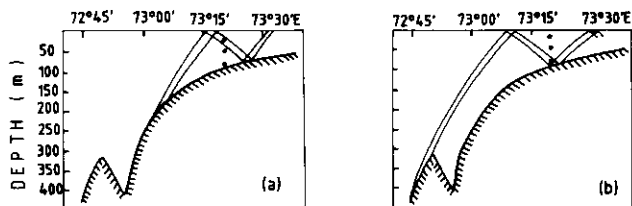


Fig. 5. Characteristics for semidiurnal frequency during May 1984.

than the barotropic components, especially in the cross-shore component. Also, the semidiurnal characteristic computed from the hydrographic data collected during the period of mooring across the shelf, combined with the distribution of phases and amplitudes of horizontal velocities, was found to be consistent with the generation of internal tides along the slope region (Fig. 5). The kinetic energy in the semidiurnal band shows a maximum at the top and bottom current meters as they were lying within the beam propagated from the slope region. The observations in the other two sets (March and November) also show a similar kinetic energy structure in the semidiurnal band. Thus, we conclude that the kinetic energy structure observed in all the three sets of observations is primarily due to similar processes (internal tides) that are accounted for by SHENOI *et al.*, (1988). Similarly, inconsistency in the distribution of horizontal kinetic energy with depth in the diurnal band may also be due to the dominant role of baroclinic tides over the shelf. However, it may be noted that the computed trajectories of rays based on hydrographic data are prone to changes due to density distribution of the water column (HAYES and HALPERN, 1976) and the mean flow generated in the water column (KROLL, 1976). The stratification of the water column during north-flowing, downwelling circulation in November is significantly different from the south-flowing, upwelling circulation off the west coast of India (SHETYE *et al.*, 1990a,b). The differences in stratification are likely to change the trajectories of rays depending on the variations in the density field. Figure 4 shows significant changes in the vertical structure of energy in the diurnal band, although the changes are not significant in the semidiurnal band.

The effects of localized land-sea breeze circulations possessing ~ 24 h periodicity are less likely to influence the diurnal peak seen in the current spectra, especially at levels close to the bottom. Since the inertial period for this location is greater than the diurnal period, it is unlikely that the upper ocean responds to the diurnal wind with an oscillatory Ekman-type circulation.

High-frequency bands 1 and 2. Variation in the horizontal kinetic energy of two high-frequency bands is also shown in Fig. 4. Comparatively low energy is observed in these bands. The drop in energy is of the order of two magnitudes from the lower frequency bands. Similar to diurnal and semidiurnal bands these high-frequency bands also show inconsistency in energy distribution with depth. Usually, the occurrence of kinetic energy, though low, in these high-frequency bands is due to the energy associated with internal waves in coastal waters (LAFOND, 1962).

Rotary coefficients

Rotary coefficients, which are an output of rotary spectral analysis, are a measure of the strength and sense of rotary motion. For currents which rotate in a circle the magnitude of

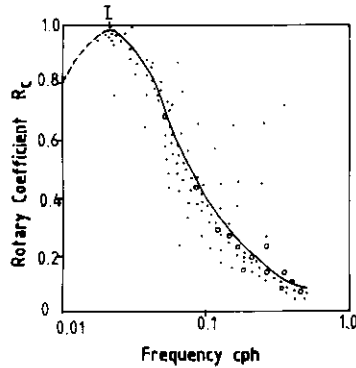


Fig. 6. Rotary coefficients for current records during March 1986. ●, Clockwise rotation; ○, anticlockwise rotation. The curve represents theoretical rotary coefficient values for internal waves.

the coefficient is unity and for unidirectional motion the coefficient is zero. The sign of the coefficient indicates the direction of rotation. Because the measurements were made in the northern hemisphere, currents due to inertial and internal wave motion are expected to rotate clockwise. The rotary coefficients for three current records during March are plotted in Fig. 6. Clockwise motion was nearly always observed for frequencies at and above local inertial frequency. Assuming an equal forcing in the clockwise and anticlockwise rotation, the theoretical rotary coefficient for internal waves (FOFONOFF, 1969) is given as

$$R_c = \frac{2\omega f}{(\omega^2 + f^2)},$$

where f is the Coriolis parameter and ω is the frequency. The theoretical curve is shown in Fig. 6. Below inertial frequency where propagating internal waves cannot occur the curve is represented by a dotted line. Above the inertial frequency where the freely propagating internal waves can occur the computed rotary coefficients from the observed current records are scattered very close to the theoretical curve given for internal waves. Thus, we conclude that above the local inertial frequency, the currents were composed mainly of internal waves.

CONCLUSIONS

This description and analysis of measured currents over the western continental shelf off Goa provide the following general characteristics of the current velocity field.

(1) The measured currents are a result of the superimposition of oscillations of wide-ranging frequencies over a weak mean flow. The mean flow was towards south during May and March and towards north during November.

(2) Inertial currents, which were concentrated near the surface, were a major contributor to the current structure.

(3) Diurnal and semidiurnal tidal frequency currents also were significant contributors to the current structure. The analysis indicates that the diurnal and semidiurnal motions were mainly due to baroclinic internal tides and not due to barotropic surface tides.

(4) Above the semidiurnal frequencies, the currents were composed mainly of high-frequency oscillations of comparatively low magnitudes.

These flow characteristics point the way for future studies of currents over the western continental shelf of India. Closely spaced arrays will be required for more detailed study of the propagation of tidal frequency internal waves.

Acknowledgements—We would like to thank Drs B. N. Desai, Director and J. S. Sastry, Deputy Director, for providing the facilities. We are also thankful to Mr A. D. Gouveia and Mr A. A. Fernandes for permitting use of their software package to compute rotary spectra. Helpful comments by two anonymous reviewers are also gratefully acknowledged.

REFERENCES

- BAINES P. G. (1973) The generation of internal tides by flat-bump topography. *Deep-Sea Research*, **20**, 179–205.
- CROW L. E., F. A. DAVIS and M. W. MAXFIELD (1960) *Statistics Manual*. Dove Publications, New York, 288 pp.
- FOFONOFF N. P. (1969) Spectral characteristics of internal waves in the ocean. *Deep-Sea Research*, **16**, 59–71.
- GONELLA J. (1972) A rotary component method for analysing meteorological and oceanographic vector time series. *Deep-Sea Research*, **19**, 833–846.
- HALPERN D., R. D. PILSBURY and R. L. SMITH (1974) An intercomparison of three current meters operated in shallow water. *Deep-Sea Research*, **21**, 489–497.
- HASTENRATH S. and P. J. LAMB (1979) *Climatic atlas of the Indian Ocean*. Part I: *Surface climate and atmospheric circulation*. Wisconsin University Press, Madison.
- HAYES S. P. and D. HALPERN (1976) Observations of internal waves and coastal upwelling off the Oregon Coast. *Journal of Marine Research*, **34**, 247–267.
- JOHNSON W. R. (1981) The propagation of tidal and inertial waves in the upwelling region off Peru. In: *Coastal upwelling*, Coastal and Estuarine Science Series No. 1, F. A. RICHARDS, editor, American Geophysical Union, Washington, DC, pp. 79–86.
- KROLL J. (1976) The effect of mean flow during an upwelling event on the rays of internal waves. *Journal of Marine Research*, **34**, 419–421.
- LAFOND E. C. (1962) Internal waves, part I. In: *The sea*, Vol. 1, M. N. HILL, editor, Interscience, New York, pp. 731–751.
- MURTY C. S. (1977) Studies on the physical aspects of shoreline dynamics at some selected places along the west coast of India. PhD thesis, University of Kerala, Kerala, 149 pp.
- POLLARD R. T. (1970) On the generation by winds of inertial waves in the ocean. *Deep-Sea Research*, **17**, 795–812.
- POLLARD R. T. and R. C. MILLARD (1970) Comparison between observed and simulated wind-generated inertial oscillations. *Deep-Sea Research*, **17**, 813–821.
- PRINSENBERG S. J. and M. RAITRAY (1975) Effects of continental slope and variable Brunt–Vaisala frequency on the coastal generation of internal tides. *Deep-Sea Research*, **22**, 251–263.
- SANDSTROM H. (1976) On topographic generation and coupling of internal waves. *Geophysical Fluid Dynamics*, **7**, 234–270.
- SHENOI S. S. C., M. K. ANTONY and D. SUNDAR (1988) Nature of the observed oscillatory flows in the shelf waters of the western continental shelf of India. *Journal of Coastal Research*, **4**, 617–626.
- SHETYE S. R. and S. S. C. SHENOI (1988) Seasonal cycle of surface circulation in the coastal north Indian Ocean. *Proceedings of Indian Academy of Sciences (Earth and Planetary Sciences)*, **97**, 53–62.
- SHETYE S. R., A. D. GOUVEIA, S. S. C. SHENOI, D. SUNDAR, G. S. MICHAEL, A. M. ALMEIDA and K. SANTANAM (1990a) Hydrography and circulation off the west coast of India during the southwest monsoon 1987. *Journal of Marine Research*, **48**, 353–378.
- SHETYE S. R., A. D. GOUVEIA, S. S. C. SHENOI, G. S. MICHAEL, D. SUNDAR, A. M. ALMEIDA and K. SANTANAM (1990b) Hydrography and circulation off the west coast of India during the Northeast monsoon 1987–88. Unpublished manuscript.
- VARKEY M. J. (1980) Power spectra of currents off Bombay. *Indian Journal of Marine Sciences*, **9**, 278–280.